Nonperiodic oscillation with wavelength of mode guided in a special Ti-diffused LiNbO3 waveguide structure

Hua, Ping-Rang; Pun, Edwin Yue-Bun; Yu, Dao-Yin; Zhang, De-Long

Published in:
IEEE Photonics Journal

Published: 01/01/2013

Document Version:
Final Published version, also known as Publisher's PDF, Publisher's Final version or Version of Record

Published version (DOI):
10.1109/JPHOT.2013.2272780

Publication details:
Hua, P-R., Pun, E. Y-B., Yu, D-Y., & Zhang, D-L. (2013). Nonperiodic oscillation with wavelength of mode guided in a special Ti-diffused $LiNbO_3$ waveguide structure. *IEEE Photonics Journal*, *5*(4), [6557425]. https://doi.org/10.1109/JPHOT.2013.2272780

IEEE Photonics Journal
An IEEE Photonics Society Publication

Open Access

Nonperiodic Oscillation With Wavelength of Mode Guided in a Special Ti-Diffused $LiNbO_3$ Waveguide Structure

Volume 5, Number 4, August 2013

Ping-Rang Hua
Edwin Yue-Bun Pun, Senior Member, IEEE
Dao-Yin Yu
De-Long Zhang

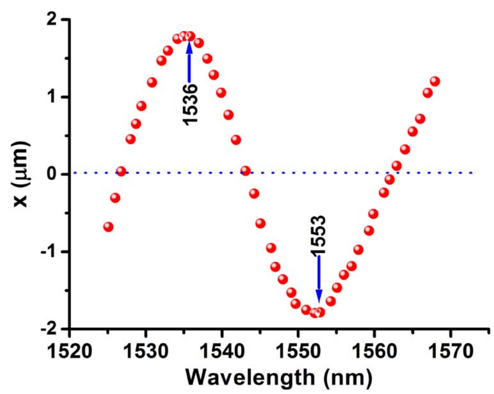

DOI: 10.1109/JPHOT.2013.2272780
1943-0655/$31.00

IEEE photonics SOCIETY

IEEE

Nonperiodic Oscillation With Wavelength of Mode Guided in a Special Ti-Diffused $LiNbO_3$ Waveguide Structure

Ping-Rang Hua,[1,2,3] **Edwin Yue-Bun Pun,**[3] ***Senior Member, IEEE,***
Dao-Yin Yu,[1,2] **and De-Long Zhang**[1,2,3]

[1]School of Precision Instruments and Opto-Electronics Engineering, Tianjin University, Tianjin 300072, China
[2]Key Laboratory of Optoelectronic Information Technology, Tianjin University, Ministry of Education, Tianjin 300071, China
[3]Department of Electronic Engineering, City University of Hong Kong, Kowloon, Hong Kong

DOI: 10.1109/JPHOT.2013.2272780
1943-0655/$31.00 ©2013 IEEE

Manuscript received May 26, 2013; revised June 29, 2013; accepted July 6, 2013. Date of publication July 11, 2013; date of current version July 16, 2013. This work was supported in part by the National Natural Science Foundation of China under Projects 61077039 and 61107056, by the Key Program for Research on Fundamental to Application and Leading Technology, Tianjin Science and Technology Commission of China under Project 11JCZDJC15500, and by the Specialized Research Fund for the Doctoral Program of Higher Education of China under Project 20100032110052. Corresponding author: D.-L. Zhang (e-mail: dlzhang@tju.edu.cn).

Abstract: We report an abnormal waveguiding phenomenon that the fundamental mode guided in strip waveguides of a special Ti-diffused $LiNbO_3$ waveguide structure, in which an array of 4- and 6-μm-wide strip waveguides is embedded in a planar waveguide, nonperiodically oscillates with the wavelength along the waveguide width direction. The oscillation amplitude reaches $\sim$2 μm. The oscillation results in a comb-like transmission spectrum at 1.5-μm wavelength region. The phenomenon is abnormal as it displays the features of multimode interference (MMI), but the single-mode pattern was captured from the strip waveguide at the 1.5-μm wavelength. Further numerical analysis for the waveguiding characteristics shows that the strip waveguide also supports a nearly cutoff higher order mode, in addition to the fundamental mode, allowing to explain the abnormal phenomenon: the MMI may take place in some regions of the strip waveguide and the observed single-mode pattern is because the higher order mode, which takes part in the MMI, is close to the cutoff.

Index Terms: Ti:$LiNbO_3$ (LN) waveguide, abnormal waveguiding characteristic, multimode interference (MMI).

1. Introduction

The concept of the special $LiNbO_3$ (LN) waveguide structure that a strip waveguide is embedded in a planar waveguide has been recently introduced. Such a special structure may find its use in developing some functional devices such as long-period waveguide grating (LPWG) and photonic crystal devices [1]–[5]. Ti-diffused LN (Ti:LN) waveguide is a fundamental component of various LN-based active or passive devices. Fully knowing the waveguiding characteristics of the special structure based upon the Ti:LN waveguide is of key importance for the design and fabrication of related devices. In the previous work, some waveguiding characteristics of such special Ti:LN waveguide structure have been studied [6]–[8]. In this paper, we report an abnormal waveguiding phenomenon in the special Ti:LN waveguide structure that an array of strip waveguides is

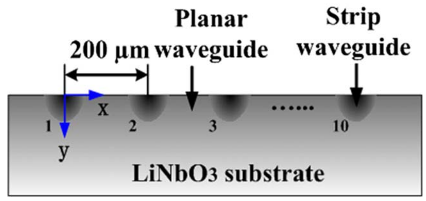

Fig. 1. Schematic of the cross section of the special Ti:LN structure of an array of 4-μm-wide 200-μm-separated strip waveguides embedded in a planar waveguide.

embedded in a planar waveguide. The fundamental transverse-magnetic (TM) mode guided in the strip waveguides nonperiodically oscillates with wavelength along the waveguide width direction. The phenomenon results in a comb-like transmission spectrum. The phenomenon looks like the multi-mode interference (MMI), but the single-mode pattern was measured from the strip waveguide. On the basis of the numerical results on the waveguiding characteristics, the abnormal phenomenon is associated with the MMI and a nearly cutoff higher order mode, which takes part in the MMI.

2. Waveguide Fabrication and Characterization

The fabrication of the special Ti:LN waveguide started from a 0.5-mm-thick Z-cut congruent LN substrate with a two-step technological process of Ti diffusion. First, a 90-nm-thick Ti metal film was coated onto one surface of the substrate followed by a diffusion at 1100 °C for 30 h in flowing argon bubbled through 20 °C water at a rate of 1.5 L/min. Second, a number of Ti strips, with the initial thickness of 100 nm and the initial widths of 4 and 6 μm, were photolithographically delineated on the surface followed by a diffusion again at 1060 °C for 8 h under the same argon atmosphere. Accordingly, a special waveguide structure of an array of strip waveguides embedded in a planar waveguide is formed. Fig. 1 shows the schematic of the cross section of the special structure of an array of 4-μm-wide 200-μm-separated strip waveguides (ten in total) embedded in a planar waveguide. For convenience, here we consider an x–y Cartesian reference frame fixed at the center of the strip waveguide surface with the x axis along the width direction and the y axis pointing to the depth. To guarantee the single-mode propagation in the width direction of the strip waveguide, a planar waveguide was introduced to weaken the lateral field confinement to the mode guided in the strip waveguide. In addition, for the LPWG application, the planar waveguide also functions as the cladding for producing the long-period grating effect.

After the fabrication, the two endfaces of the sample were optically polished to facilitate the end-fire coupling. The final length of the waveguides is 1.5 cm. The end-fire experiment was carried out by launching into the strip waveguides the polarized light emitted from a tunable laser with a bandwidth of 1525–1570 nm via endface butt-coupling between a section of polarization-maintaining single-mode fiber (Thorlabs Panda PM 1550-HP with a mode field diameter of 10.5 $\pm$ 0.4 μm) and one channel waveguide. A polarization controller (Optics for Research, Inc.) was used to control the state of polarization of the light launched into the waveguide. The magnified near-field image of guided TM or transverse-electric (TE) mode was projected onto a LBA-USB-L130-1550 infrared charge-coupled device camera (OPHIR-Spiricon, Inc.) through a 40 $\times$ microscope objective lens. To increase the spatial resolution, a microscope objective lens with a larger numerical aperture of 0.65 was employed. The camera has a spectral response range of 1440–1605 nm and an effective pixel number of 1392 $\times$ 1040 with a pixel pitch 3.2 μm in the lateral direction and 4.3 μm in the vertical direction. The transmission spectrum of the strip waveguide was measured by butt-coupling out the guided light using a pigtailed fiber and detecting with an optical spectrum analyzer. An erbium-doped fiber amplifier (EDFA) with a bandwidth of 1520–1580 nm was used as the light source.

3. Results and Discussion

End-fire coupling experiment shows that waveguiding exists in all strip waveguides. Both TM and TE modes are guided. It appears that all waveguides support single-mode propagation. Fig. 2

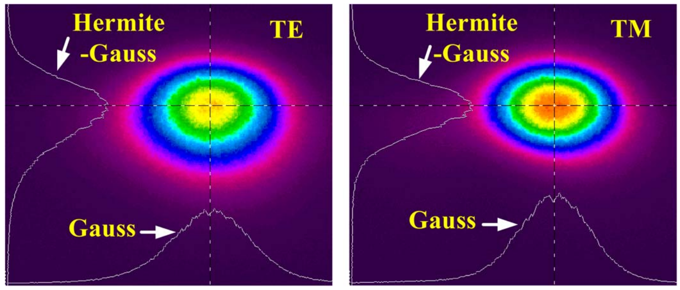

Fig. 2. Near-field patterns and profiles of TE and TM modes guided in the 4-μm-wide strip waveguide of the special Ti:LN waveguide structure at the 1545-nm wavelength.

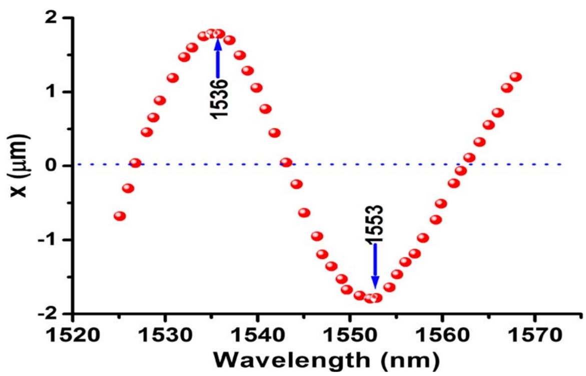

Fig. 3. Wavelength dependence of *x* coordinate of the center of TM mode guided in the 4-μm-wide strip waveguide of the special Ti:LN waveguide structure.

shows the patterns of TE and TM modes guided in the 4-μm-wide strip waveguide at the 1545-nm wavelength. As expected, the waveguides confine the TM mode strongly, whereas the TE mode weakly. Analysis shows that the light intensity of both the TE and TM modes guided in the strip waveguides follows a Gauss function $A_x \exp[-2(x/W_x)^2]$ in the width direction *x* and a Hermite–Gauss function $A_y y^2 \exp[-2(y/W_y)^2]$ in the depth direction *y*. The fitting mode sizes W_x and W_y are 5.8 and 6.0 ± 0.2 μm for the TE, and 4.7 and 3.6 ± 0.2 μm for the TM mode guided in the 4-μm-wide strip waveguide.

The propagation loss at the 1.5-μm wavelength was evaluated for both TE and TM modes in the 4-μm-wide strip waveguide from the reflection loss, measured insertion loss, and coupling loss evaluated from the known mode size. The fiber-to-fiber insertion loss of the 1.5-cm-long 4-μm-wide waveguide was measured to be 3.2 dB for the TE mode and 5.9 dB for the TM mode. From the measured mode sizes, the coupling loss between the 4-μm-wide waveguide and the polarization-maintaining single-mode fiber (with a mode field diameter of 10.5 ± 0.4 μm) is similar to 2.2 dB for the TE mode and 5.2 dB for the TM mode. With ignored etalon effect, the total reflection loss of the two waveguide endfaces against the two fiber endfaces is ~ 0.3 dB for both cases of TM and TE polarizations. The propagation loss is then evaluated as 0.5 and 0.3 dB/cm for the TE and TM mode, respectively.

By utilizing the tunable laser, we are able to capture the near-field mode patterns under different working wavelengths and quantify the wavelength dependence of *x* coordinate of the center of the TM single mode guided in the strip waveguides of the special waveguide structure. The coordinate is calibrated by the spatial resolution (length per pixel) determined from the captured mode pattern of input single-mode fiber, which has the known mode field diameter of 10.5 ± 0.4 μm. Fig. 3 shows the result of the 4-μm-wide strip waveguide. As the wavelength is changed, the TM mode oscillates along the waveguide width direction *x*. Due to the limited bandwidth of 1525–1570 nm of the

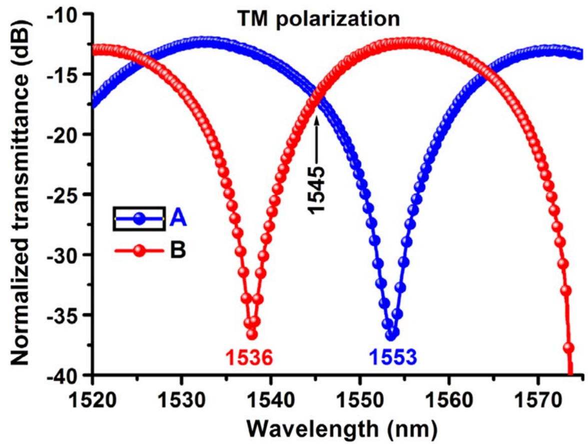

Fig. 4. Normalized transmission spectra of the 4-μm-wide strip waveguide of the special Ti:LN waveguide structure. Spectra A and B were measured by aligning the output fiber to the two x coordinates corresponding to the positive and negative maximum shifts indicated in Fig. 3.

tunable laser, only one period could be obtained. The oscillation amplitude reaches 1.8 ± 0.3 μm, which takes place at the wavelengths of 1536 and 1553 nm. The peak-to-peak interval is $\sim$34 nm. Further check shows that the oscillation is not strictly periodic. Aiming at $x = \pm 1.8 \pm 0.3$ μm, we have measured the transmission spectra of the 4-μm-wide strip waveguide. It was done by simply aligning the output fiber to $x = \pm(1.8 \pm 0.3)$ μm, whereas the input fiber remaining at the position where Fig. 3 was obtained. The results are shown in Fig. 4. Spectrum A (B) corresponds to the case that the output fiber was positioned at the x coordinate of positive (negative) maximum shift, which takes place at the wavelength 1536 (1553) nm (see Fig. 3). One can see that the dip on spectrum A (B) appears at 1553 (1536) nm with an extinction ratio -24 (-24) dB and a 3-dB bandwidth of $\sim$20 (18) nm. Again, due to the limitation by the bandwidth of EDFA (1520–1580 nm), only one more period could be measured, and the dips do not show the strict periodicity. The peak-to-peak interval is evaluated to be 34 nm, which agrees well with the result evaluated from Fig. 3. Next, we try to explain the spectral feature in Fig. 4. Fig. 3 implies that different excitation wavelengths correspond to different propagation paths. As a result, at a given waveguide output endface, the modes with different wavelengths center at different x positions. In this case that the output fiber was positioned at $x = -(1.8 \pm 0.3)$ μm, the 1553-nm light is detected, whereas the 1536-nm light is not detected. As a result, a dip at 1536 nm is observed in spectrum B, as shown in Fig. 4. The feature of spectrum A can be explained in a similar way.

Some additional experiments were done with regard to the observed waveguiding characteristic. The results show that the waveguiding characteristic does not depend on the x coordinate of the input fiber. The phenomenon is observed whether the input fiber was aligned at the optimum position of input-coupling (i.e., $x = 0$) or not. Similar phenomenon was also observed for the strip waveguides with the 6-μm initial Ti-strip width. However, the dip position in the transmission spectrum changes from an initial Ti-strip width to another. On the other hand, the phenomenon could not be observed under the TE polarization. It cannot be observed also for the strip waveguide on the substrate with an array of 200 μm-separated strip waveguides without the planar waveguide. In addition, we have also studied the thermal effect of the phenomenon over the temperature range of 20–70 $^\circ$C. The result shows that the phenomenon is temperature independent.

Next, we try to discuss the physics behind the phenomenon. First of all, we can exclude several possibilities, such as the coupling between the strip and the planar waveguides (because the light power does not lose from the strip waveguide except for the usual waveguide loss), the coupling among the strip waveguides (because the separation each other is large enough, i.e., 200 μm), and the interaction between the TE and TM modes. The observed waveguiding characteristic is very similar to that of MMI, which was observed in a usual multimode Ti:LN strip waveguide [9], [10]. However, the waveguiding characteristic here appears to take place in a single-mode waveguide.

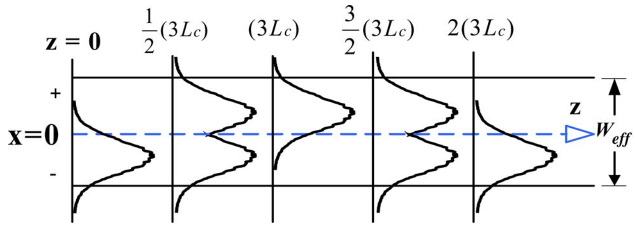

Fig. 5. Model for evolution along the propagation direction *z* of TM mode field profile in the width direction of the usual MMI strip waveguide.

The phenomenon is thus abnormal. A discussion in comparison with the usual MMI is helpful for understanding the phenomenon. Fig. 5 depicts the evolution along the propagation direction *z* of TM mode field distribution in the width direction of the usual MMI Ti:LN strip waveguide. W_{eff} and L_c denote the effective waveguide width and the wavelength-dependent coupling length between the two lowest order modes in the waveguide, respectively, and $L_c \approx 4N_{eff}(W_{eff})^2/(3\lambda)$ [9], where N_{eff} and λ are the effective refractive index and the wavelength of input beam, respectively. For a given wavelength, the input field profile is reproduced in single-mode or two-mode image at periodic intervals along the propagation direction *z*. As shown in Fig. 5, the single-mode image appears at $z = 3L_c$ and $2(3L_c)$, and the two-mode image appears at $z = 3L_c/2$ or $3(3L_c)/2$. These features of MMI imply that the strip waveguides studied here may be multimode also. Two possible factors may result in the observation of the single-mode pattern.

One possible factor is that the observed single-mode pattern was captured just at $z = 3nL_c$ $(n = 1, 2, 3, \ldots)$. We have expended a great effort to make this argument clear. Obviously, it is not easy to do it by alternatively doing the sample cutting and the mode pattern capture. The argument is actually clarified by selecting an adequate working wavelength (1545 nm here) and capturing the mode pattern (see Fig. 2). The reason is detailed in the succeeding discussion. If the phenomenon originates from the MMI, the single-mode image should be observed for the 1536- or 1553-nm working wavelength because all of the light propagates and centers at the *x* coordinate of either positive or negative maximum shift. Away from the two wavelengths, the light propagates at both sides of positive and negative coordinates, and a two-mode pattern is expected. This feature should be most evident for the 1545-nm wavelength because it is the median of 1536 and 1553 nm. As shown in Fig. 2, the single-mode image was captured. The same result is obtained as the wavelength is detuned from the 1536 or 1553 nm and continuously changed within the available wavelength range of 1525–1570 nm. This is also the case as the position of the input fiber is changed. Thus, we can rule out the factor that the observed single-mode pattern was captured just at $z = 3nL_c$ $(n = 1, 2, 3, \ldots)$.

Another possible factor for the observation of the single-mode pattern is that the waveguide supports a nearly cutoff higher order mode. Perhaps, in some regions, the waveguide support a higher order mode, and the MMI takes place there. Because the higher order mode approaches the cutoff, its mode pattern cannot be resolved. It is thus essential to have the information about the cutoff condition of the higher order modes possibly guided in the special structure under study. The information can be obtained by doing a numerical analysis for the waveguiding characteristics. With regard to the special waveguide structure studied here, the 2-D ordinary or extraordinary index profile $n(x, y)$ in the strip waveguide region is assumed as the simple overlap of the profiles of the planar and strip waveguides. Under the Cartesian reference frame given in Fig. 1, it can be expressed as

$$n(x, y) = n_b + \Delta n_1 \exp\left[-(y/d_y)\right]^2 + 0.5\Delta n_2\{\mathrm{erf}[(W + 2x)/(2d_x)] + \mathrm{erf}[(W - 2x)/(2d_x)]\} \times \exp\left[-(y/d'_y)^2\right]/\mathrm{erf}[W/(2d_x)] \quad \text{for } -\infty < x < +\infty \text{ and } y \geq 0, \quad (1)$$

where the first term represents the substrate index, the second term denotes the contribution of the planar waveguide, and the third term reflects the contribution of the strip waveguide. Δn_1 and Δn_2 are

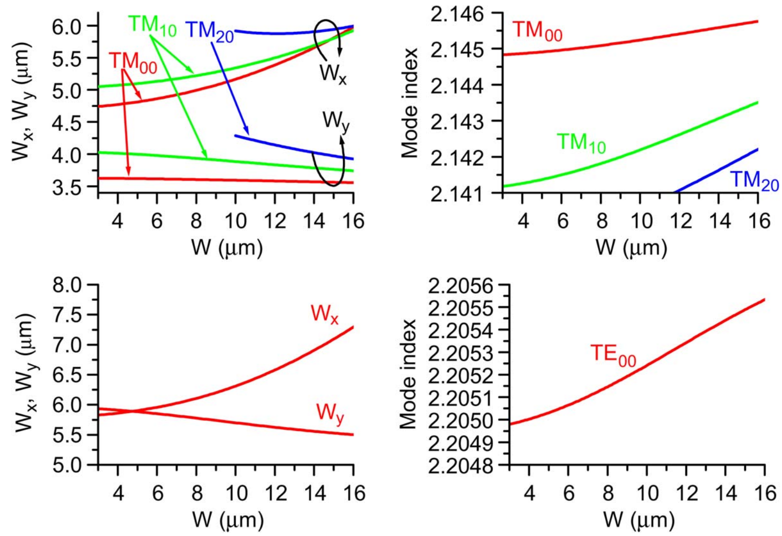

Fig. 6. Calculated mode sizes W_x and W_y, and effective refractive index (at 1.53-μm wavelength) as a function of initial Ti-strip width W for the three lowest order TM_{n0} and TE_{n0} ($n = 0$, 1, and 2) modes that are possibly guided in the strip waveguides of the special waveguide structure fabricated.

the Ti-induced surface index increments corresponding to the homogeneously coated Ti film (90 nm thick here) and the photolithographically patterned Ti strip (100 nm thick here), respectively. W is the initial Ti-strip width. Parameter d_x is the width of the strip waveguide, and d_y and d_y' are the depths of the planar and strip waveguides, respectively. Aiming at the waveguide structure fabricated here, we have calculated the mode sizes (W_x and W_y) and the effective index N_{eff} of three lowest order TM_{n0} and TE_{n0} ($n = 0$, 1, and 2) modes, which are possibly guided in the strip waveguides, as a function of W from 3 to 16 μm using the variational method [8]. The simulation aimed at the 1.53-μm wavelength, at which the substrate index is 2.1380 (2.2035) for the extraordinary (ordinary) ray. The other input parameters under the diffusion condition adopted are evaluated according to Refs. [11]–[13]. Fig. 6 shows the numerical results of the mode sizes and effective indexes. First of all, it is essential to compare the numerical results with the experimental data. For the 4-μm-wide strip waveguide, the calculated mode sizes W_x and W_y are 5.9 and 5.9 μm for the fundamental TE mode (TE_{00}), and 4. 8 and 3.6 μm for the fundamental TM mode (TM_{00}), which are in good agreement with the experimental results, 5.8 and 6.0 ± 0.2 μm for the TE_{00} mode, and 4.7 and 3.6 ± 0.2 μm for the TM_{00} mode. The good agreement between theory and experiment implies that the refractive index model proposed for the special structure studied here is close to the practical scenario. Next, we pay attention to the mode cutoff condition. As we know, the criterion for the waveguiding is that the mode index N_{eff} is larger than the substrate index. For the usual planar or strip waveguide, it is easy to determine the mode cutoff condition using this criterion. This is the case for the planar waveguide of the special structure studied here as the substrate index is simply the index of the bulk material n_b. For the strip waveguide of this special structure, however, it is not easy to determine the mode cutoff condition because the substrate index is no longer the n_b but the sum of the n_b and the index increment of the planar waveguide. This means that, for the strip waveguide here, the substrate index varies along the depth direction with a maximum value $n_b + \Delta n_1$ at the waveguide surface. In this case, the criterion for the waveguiding should be that the mode index N_{eff} is larger than the $n_b + \Delta n_1$, which has a value of 2. 1410 (2.2048) for the extraordinary/ordinary ray at the 1.53-μm wavelength [Note that, for a waveguide on a Z-cut LN substrate, the TM (TE)-mode concerns the extraordinary (ordinary) index]. Based upon this criterion and the N_{eff}-W plots in Fig. 6, we can readily judge the cutoff condition of the higher order modes TM_{n0} and TE_{n0} possibly guided in the strip waveguides under study. Under the TE polarization, the strip waveguide only supports the fundamental mode TE_{00} and all of the higher order modes are cutoff even if the waveguide has an initial Ti-strip width as wide as 16 μm. It is thus reasonable that the MMI phenomenon is not observed under the TE polarization. Under the TM polarization, however, the strip waveguide even with an initial Ti-strip width as narrow as 3 μm also supports the second-order mode TM_{10}, aside the fundamental mode TM_{00}. Just as guessed above, while the fundamental mode TM_{00} being well guided, the TM_{10} mode is close to the cutoff region for $W < 6$ μm. It is thus comprehensive that the MMI features are observed under the TM polarization, and while the TM_{00} mode pattern being well resolved, the TM_{10} mode pattern cannot be resolved.

4. Conclusion

We have demonstrated an abnormal waveguiding characteristic in single-mode Ti:LN strip waveguides embedded in a Ti:LN planar waveguide. It is found that the TM mode guided in the strip waveguides nonperiodically oscillates with the wavelength along the waveguide width direction. Different excitation wavelengths correspond to different propagation paths. As a result, at a given waveguide output endface, the modes with different wavelengths center at different *x* positions, and a comb-like transmission spectrum is obtained. The phenomenon is abnormal as it displays the MMI features, but the single-mode image was captured from the strip waveguide. Further numerical analysis for the waveguiding characteristics shows that the strip waveguide also supports a nearly cutoff higher order mode, aside the fundamental mode. This result allows to explain the abnormal observation. In some regions of the strip waveguide, the MMI may take place. In other words, the abnormal phenomenon may result from the MMI. The observed single-mode image is because the higher order mode, which takes part in the MMI, is close to the cutoff.

References

[1] W. Jin, K. S. Chiang, and Q. Liu, "Electro-optic long-period waveguide gratings in lithium niobate," *Opt. Exp.*, vol. 16, no. 25, pp. 20 409–20 417, Dec. 2008.

[2] W. Jin, K. S. Chiang, and Q. Liu, "Thermally tunable lithium-niobate long-period waveguide grating filter fabricated by reactive ion etching," *Opt. Lett.*, vol. 35, no. 4, pp. 484–486, Feb. 2010.

[3] P. R. Hua, D. L. Zhang, and E. Y. B. Pun, "Long-period grating on strip Ti:$LiNbO_3$ waveguide embedded in planar Ti:$LiNbO_3$ waveguide," *IEEE Photon. Technol. Lett.*, vol. 22, no. 18, pp. 1361–1363, Sep. 2010.

[4] G. W. Burr, S. Diziain, and M. P. Bernal, "The impact of finite-depth cylindrical and conical holes in lithium niobate photonic crystals," *Opt. Exp.*, vol. 16, no. 9, pp. 6302–6316, Apr. 2008.

[5] M. Roussey, M. P. Bernal, N. Courjal, and F. I. Baida, "Experimental and theoretical characterization of a lithium niobate photonic crystal," *Appl. Phys. Lett.*, vol. 87, no. 24, pp. 241101-1–241101-3, Dec. 2005.

[6] P. R. Hua, B. Chen, Q. Z. Zhao, F. Han, D. Y. Yu, E. Y. B. Pun, and D. L. Zhang, "Shallow Ti:$LiNbO_3$ strip waveguide," *IEEE Photon. J.*, vol. 4, no. 2, pp. 520–527, Apr. 2012.

[7] B. Chen, P. R. Hua, S. Y. Xu, D. Y. Yu, E. Y. B. Pun, and D. L. Zhang, "Mode indices measurement of a special Ti-diffused $LiNbO_3$ waveguide structure: A strip waveguide array embedded in a planar waveguide," *IEEE Photon. J.*, vol. 4, no. 5, pp. 1553–1559, Oct. 2012.

[8] D. L. Zhang, S. Zhang, P. R. Hua, D. Y. Yu, and E. Y. B. Pun, "A theoretical study on special Ti:$LiNbO_3$ structure of an array of strip waveguides embedded in a planar waveguide," *J. Lightwave Technol.*, vol. 30, no. 23, pp. 3653–3659, Dec. 2012.

[9] Y. L. Lee, Y. W. Choi, H. S. Jung, T. J. Eom, W. Shin, D. K. Ko, W. S. Yang, H. M. Lee, W. K. Kim, and H. Y. Lee, "Temperature-insensitive dual-comb filter based on multi-mode interference Ti:$LiNbO_3$ waveguide," *IEEE Photon. Technol. Lett.*, vol. 21, no. 8, pp. 507–509, Apr. 2009.

[10] Y. L. Lee, T. J. Eom, W. Shin, B. A. Yu, D. K. Ko, W. K. Kim, and H. Y. Lee, "Characteristics of a multi-mode interference device based on Ti:$LiNbO_3$ channel waveguide," *Opt. Exp.*, vol. 17, no. 13, pp. 10 718–10 724, Jun. 2009.

[11] M. Fukuma and J. Noda, "Optical properties of titanium-diffused $LiNbO_3$ strip waveguides and their coupling-to-a-fiber characteristics," *Appl. Opt.*, vol. 19, no. 4, pp. 591–597, Feb. 1980.

[12] S. Fouchet, A. Carenco, C. Daguet, R. Guglielmi, and L. Riviere, "Wavelength dispersion of Ti induced refractive index change in $LiNbO_3$ as a function of diffusion parameters," *J. Lightwave Technol.*, vol. 5, no. 5, pp. 700–708, May 1987.

[13] E. Strake, G. P. Bava, and I. Montrosset, "Guided modes of Ti:$LiNbO_3$ channel waveguides: A novel quasi-analytical technique in comparison with the scalar finite-element method," *J. Lightwave Technol.*, vol. 6, no. 6, pp. 1126–1135, Jun. 1988.